Covalent versus ionic bonding in alkalimetal fluoride oligomers

ARTICLE *in* JOURNAL OF COMPUTATIONAL CHEMISTRY · JANUARY 2007

Impact Factor: 3.59 · DOI: 10.1002/jcc.20547 · Source: PubMed

3 AUTHORS:

F. Matthias Bickelhaupt
VU University Amsterdam
375 PUBLICATIONS **10,947** CITATIONS
SEE PROFILE

Miquel Solà
Universitat de Girona
395 PUBLICATIONS **8,501** CITATIONS
SEE PROFILE

Célia Fonseca Guerra
VU University Amsterdam
151 PUBLICATIONS **7,483** CITATIONS
SEE PROFILE

Covalent *Versus* Ionic Bonding in Alkalimetal Fluoride Oligomers

F. M. BICKELHAUPT,[1] M. SOLÀ,[2] C. FONSECA GUERRA[1]

[1]*Afdeling Theoretische Chemie, Scheikundig Laboratorium der Vrije Universiteit, De Boelelaan 1083, NL-1081 HV Amsterdam, The Netherlands*

[2]*Institut de Química Computacional, Universitat de Girona, Campus Montilivi, E-17071 Girona, Catalonia, Spain*

Received 12 May 2006; Accepted 9 June 2006
DOI 10.1002/jcc.20547
Published online in Wiley InterScience (www.interscience.wiley.com).

Abstract: The most polar bond in chemistry is that between a fluorine and an alkalimetal atom. Inspired by our recent finding that other polar bonds (C—M and H—M) have important covalent contributions (i.e., stabilization due to bond overlap), we herein address the question if covalency is also essential in the F—M bond. Thus, we have theoretically studied the alkalimetal fluoride monomers, FM, and (distorted) cubic tetramers, $(FM)_4$, with M = Li, Na, K, and Rb, using density functional theory at the BP86/TZ2P level. Our objective is to determine how the structure and thermochemistry (e.g., F—M bond lengths and strengths, oligomerization energies, etc.) of alkalimetal fluorides depend on the metal atom, and to understand the emerging trends in terms of quantitative Kohn–Sham molecular orbital theory. The analyses confirm the extreme polarity of the F—M bond (dipole moment, Voronoi deformation density and Hirshfeld atomic charges), and they reveal that bond overlap-derived stabilization (ca. −6, −6, and −2 kcal/mol) contributes only little to the bond strength (−136, −112, and −114 kcal/mol) and the trend therein along Li, Na, and K. According to this and other criteria, the F—M bond is not only strongly polar, but also has a truly ionic bonding mechanism. Interestingly, the polarity is reduced on tetramerization. For the lithium and sodium fluoride tetramers, the F_4 tetrahedron is larger than and surrounds the M_4 cluster (i.e., F—F > M—M). But in the potassium and rubidium fluoride tetramers, the F_4 tetrahedron is smaller than and inside the M_4 cluster (i.e., F—F < M—M).

 J Comput Chem 28: 238–250, 2007

Key words: alkalimetals; bonding theory; covalency; fluorine; ionicity; polar bonds

Introduction

About one century ago, Lewis introduced the idea of the electron-pair bond. On page 767, it is pointed out in a footnote that the basic ideas of the theory (in particular the "cubical atom") were developed by Lewis already in the year 1902.[1] According to postulate 3 of his model, a stable configuration arises when two atoms combine, such that they adopt what is nowadays called the noble-gas configuration by sharing a pair of electrons (**1**). In the same publication, he also proposed to replace the classification of substances into inorganic and organic by one into polar and nonpolar. In a polar bond, the shared electron pair is shifted closer to the more (electro)negative atom (**2**).

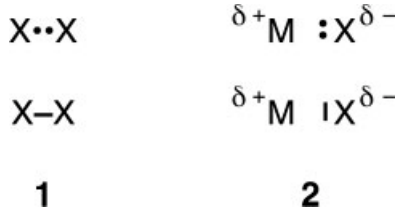

1 **2**

Herein, we focus on the alkalimetal–halogen bond. This is the most polar of all chemical bonds, and small oligomers of alkalimetal halides are therefore attractive systems for studying the nature of highly polar bonds. Alkalimetal halide molecules and clusters $(XM)_n$ (X = halogen and M = alkalimetal) occur in

Correspondence to: F. M. Bickelhaupt; e-mail: FM.Bickelhaupt@few.vu.nl; or M. Solà; e-mail: miquel.sola@udg.es

Contract/grant sponsor: HPC-Europa Program of the European Union

Contract/grant sponsor: Deutsche Akademische Austauschdienst (DAAD)

Contract/grant sponsor: Netherlands Organization for Scientific Research (NWO)

Contract/grant sponsor: Ministerio de Educación y Ciencia (MEC)

Contract/grant sponsor: Training and Mobility of Researchers (TMR) Program of the European Union

Contract/grant sponsor: DURSI (Generalitat de Catalunya)

Contract/grant sponsor: National Research School Combination–Catalysis (NRSC-C)

hot vapors of these materials,[2] and their investigation provides valuable insight into how physicochemical properties evolve going from molecular systems to the solid state. Thus, various experimental[2,3] and theoretical[4,5] studies have been devoted to obtaining structural and thermochemical data about these species. Particularly, compact and stable clusters $(XM)_n$ arise for the so-called magic numbers: $n = 4$, 6, 9, 12, 15, and 18.[2a] These clusters exist in various isomeric forms that may be in thermal equilibrium with each other. The tetramer $(XM)_4$, for example, occurs among other as cube (**3**), ladder (**4**), and ring (**5**),[2a] the cubic isomer (**3**) being typically (but not always) the most stable form.[4b,5(c,k)]

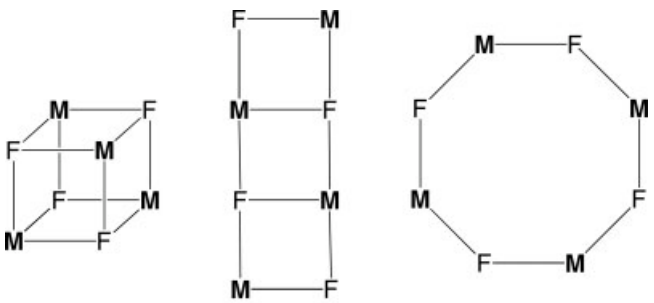

The purpose of the present study is twofold. First, we aim at a better understanding of the nature of the most polar bond in chemistry, that is, the bond between fluorine and an alkalimetal. This is inspired by the recent finding that the C—M and H—M bond have unexpectedly substantial covalent character (which is essential for understanding trends in bond strengths) and by the insight that one must distinguish between covalent or ionic features in the bonding mechanism on one hand and the polarity of the charge distribution on the other hand.[6] In particular, the question is to what extent the stabilization of bringing a neutral alkalimetal and fluorine atom together is (still) caused by bond overlap between the atomic orbitals (AOs) (i.e., constructive interference of the two atomic wavefunctions) besides the ionic stabilization that arises from transferring the electron of the high-energy metal AO to the low-energy fluorine AO. Or, to cast this in terms of the Lewis model, we wish to know to what extent the mechanism that is responsible for providing the stabilization associated with the shared-electron bond in **1**, which is also contributing to the stability of the highly polar situation **2** as it exists in alkalimetal fluorides. It is interesting to note in this context that a categorization of the bonding mechanism into bond-overlap driven (i.e., inducing a stabilization by reducing the kinetic-energy pressure along the bond axis) and driven by a difference in electronegativity across the bond also arises from the analysis of the bond energy ΔE in terms of the electron kinetic energy component ΔT_e, the electron–nuclear attraction component ΔV_{ne}, and the electron–electron repulsion ΔV_{ee} (for a detailed didactic account of the latter approach, see the article by Bitter et al. in the same issue).[7]

We have undertaken a detailed investigation of alkalimetal fluoride monomers FM and tetramers $(FM)_4$ with M = Li, Na, K, and Rb, using the generalized gradient approximation (GGA) of density functional theory (DFT) at the BP86/TZ2P level of theory.[8] The polar F—M bonds are analyzed in the framework of the Kohn–Sham molecular orbital (KS-MO) model, using a quantitative bond energy decomposition.[8] Our analyses reveal that, at variance with the C—M bond, the F—M bond has not only a strongly polar charge distribution but also a dominantly ionic bonding mechanism.

A second objective is to obtain a set of consistent structural and thermochemical data for alkalimetal fluoride monomers FM and tetramers (geometries, F—M bond strengths, tetramerization energies), all obtained with exactly the same GGA density functional method. This complements the available experimental and theoretical data, which are scarce or missing for the tetramers of the heavier alkalimetal systems (beyond lithium), and enables a systematic analysis of the trends. In this context, we note that obtaining experimental information on the tetramers is difficult; only $(FLi)_4$ has been detected as a matrix-isolated molecule in rare-gas matrices.[4d] For the tetramers, we focus on the most stable, i.e., the cubic isomer, which is in general not a perfect but a distorted cube. In $(FLi)_4$, for example, the lithium atoms constitute an inner cluster that is surrounded by four fluorine atoms, one on each face of the tetrahedral metal cluster, similar to the situation for tetramethyllithium.[6b] A striking structural phenomenon that we find is the change of relative size of the fluoride tetrahedron and the metal cluster if one goes from sodium to potassium. Thus, for the heavier alkalimetals K and Rb, the F_4 unit is inside the M_4 cluster.

Theoretical Methods

General Procedure

All calculations were performed using the Amsterdam Density Functional program.[9] The numerical integration was carried out using the procedure developed by Baerends and coworkers.[9(e,f)] The molecular orbitals (MOs) were expanded in a large uncontracted set of Slater-type orbitals (STOs) containing diffuse functions, which is of triple-ζ quality for all atoms and has been augmented with two sets of polarization functions: 3d and 4f on F, Li, and Na; 4d and 4f on K and Rb.[9g] In addition, an extra set of p functions was added to the basis sets of Li (2p), Na (3p), K (4p), and Rb (5p). The 1s core shell of fluorine and lithium, the 1s 2s 2p core shells of sodium and potassium, and the 1s 2s 3s 2p 3p 3d core shells of rubidium were treated by the frozen-core approximation.[9d] An auxiliary set of s, p, d, f, and g STOs was used to fit the molecular density and to represent the Coulomb and exchange-correlation potentials accurately in each SCF cycle.[9h]

Energies, geometries,[10] and frequencies[11] were computed using the GGA of DFT at the BP86 level.[12] All open-shell systems were treated with the spin-unrestricted formalism. All species were confirmed to be equilibrium structures, i.e., the number of vibrational normal modes associated with an imaginary frequency is zero. Bond enthalpies at 298.15 K and 1 atm

(ΔH_{298}) were calculated from electronic bond energies (ΔE) according to eq. (1), assuming an ideal gas.[13]

$$\Delta H_{298} = \Delta E + \Delta E_{\text{trans.298}} + \Delta E_{\text{rot.298}} + \Delta E_{\text{vib,0}} + \Delta(\Delta E_{\text{vib,0}})_{298} + \Delta(pV). \quad (1)$$

Here, $\Delta E_{\text{trans,298}}$, $\Delta E_{\text{rot,298}}$, and $\Delta E_{\text{vib,0}}$ are the differences between products and reactants in translational, rotational, and zero point vibrational energy, respectively; $\Delta(\Delta E_{\text{vib}})_{298}$ is the change in the vibrational energy difference as one goes from 0 to 298.15 K. The vibrational energy corrections are based on our frequency calculations. The molar work term $\Delta(pV)$ is $(\Delta n)RT$ (e.g., for two fragments combining to one molecule $\Delta n = -1$). Thermal corrections for the electronic energy are neglected.

Bond Energy Decomposition

The overall bond energy ΔE is made up of two major components [eq.(2)]:

$$\Delta E = \Delta E_{\text{prep}} + \Delta E_{\text{int}}. \quad (2)$$

In this formula, the preparation energy ΔE_{prep} is the energy needed to deform the separate molecular fragments from their equilibrium structure to the geometry that they attain in the overall molecular system. The interaction energy ΔE_{int} is the energy released when the prepared fragments are brought together into the position they have in the overall molecule. It is analyzed for our model systems in the framework of the KS-MO model, using a Morokuma-type decomposition into electrostatic interaction, Pauli repulsion (or exchange repulsion), and (attractive) orbital interactions [eq. (3)].[8,14]

$$\Delta E_{\text{int}} = \Delta V_{\text{clst}} + \Delta E_{\text{Pauli}} + \Delta E_{\text{oi}}. \quad (3)$$

The term ΔV_{elstat} corresponds to the classical electrostatic interaction between the unperturbed charge distributions of the prepared (i.e. deformed) fragments and is usually attractive. The Pauli-repulsion, ΔE_{Pauli}, comprises the destabilizing interactions between occupied orbitals and is responsible for the steric repulsion. The orbital interaction ΔE_{oi} in any MO model, and therefore also in Kohn–Sham theory, accounts for electron-pair bonding, charge transfer (i.e., donor–acceptor interactions between occupied orbitals on one fragment with unoccupied orbitals of the other, including the HOMO-LUMO interactions), and polarization (empty-occupied orbital mixing on one fragment due to the presence of another fragment). In case of open-shell fragments, the bond energy analysis yields, for technical reasons, interaction energies that differ consistently in the order of kcal/mol from the exact BP86 result. To facilitate a straightforward comparison, the results of the bond energy analysis were scaled to match exactly the regular BP86 bond energies.

The orbital interaction energy can be decomposed into the contributions from each irreducible representation Γ of the interacting system [eq. (4)], using the extended transition state scheme developed by Ziegler and Rauk.[14(d,e)]

$$\Delta E_{\text{oi}} = \sum_{\Gamma} \Delta E_{\Gamma}. \quad (4)$$

Analysis of the Charge Distribution

The electron density distribution is analyzed using the Voronoi deformation density (VDD) method[15,16] and the Hirshfeld scheme[17] for computing atomic charges. The VDD atomic charge $Q_{\text{A}}^{\text{VDD}}$ is computed as the (numerical) integral[9f] of the deformation density $\Delta\rho(\mathbf{r}) = \rho(\mathbf{r}) - \sum_{\text{B}} \rho_{\text{B}}(\mathbf{r})$ in the volume of the Voronoi cell of atom A [eq. (5)]. The Voronoi cell of atom A is defined as the compartment of space bounded by the bond midplanes on and perpendicular to all bond axes between nucleus A and its neighboring nuclei (cf. the Wigner–Seitz cells in crystals[16c]).

$$Q_{\text{A}}^{\text{VDD}} = -\int_{\text{Voronoi cell of A}} \left(\rho(\mathbf{r}) - \sum_{\text{B}} \rho_{\text{B}}(\mathbf{r})\right) \mathbf{dr}. \quad (5)$$

Here, $\rho(\mathbf{r})$ is the electron density of the molecule and $\sum_{\text{B}}\rho_{\text{B}}(\mathbf{r})$ the superposition of atomic densities ρ_{B} of a fictitious promolecule without chemical interactions that is associated with the situation in which all atoms are neutral. The interpretation of the VDD charge $Q_{\text{A}}^{\text{VDD}}$ is rather straightforward and transparent. Instead of measuring the amount of charge associated with a particular atom A, $Q_{\text{A}}^{\text{VDD}}$ directly monitors how much charge flows, due to chemical interactions, out of ($Q_{\text{A}}^{\text{VDD}} > 0$) or into ($Q_{\text{A}}^{\text{VDD}} < 0$) the Voronoi cell of atom A, that is, the region of space that is closer to nucleus A than to any other nucleus.

Results and Discussion

Structures

Monomers

The computed BP86/TZ2P geometries are summarized in Table 1 and, for the tetramers, illustrated in Figure 1. The F—M bond distance in the diatomic alkalimetal fluoride monomers increases systematically from 1.615 to 2.000, to 2.296 to 2.397 Å along M = Li, Na, K, and Rb, respectively. Note that the increase in bond length in every step becomes smaller as one descends the periodic table.

This trend agrees well with earlier theoretical work[5(a,d,g–l)] and microwave[3(c,d,g,h)] and electron diffraction[3a] experiments, which also yield a monotonic increase of the F—M bond along FLi, FNa, FK, and FRb (note that there is no other theoretical study that treats the whole series consistently at the same level of theory). The experimental (microwave) bond lengths are, however, systematically shorter by 3–5% than our BP86/TZ2P and most other theoretical values. The nearly exact agreement between Hartree–Fock and experiment in case of FLi and FNa is probably fortuitous.

Tetramers

Tetramerization causes the F—M bond to expand by ~0.25 Å for all alkalimetals studied (Table 1). Thus, the F—M bond in

Table 1. Structures (in Å) of Alkalimetal Fluoride Monomers and Tetramers.

Method	F—M	M—M	F—F	Ref.
FLi				
BP86/TZ2P	1.615	–	–	This work
HF/6-311++G(2d,2p)	1.565	–	–	5l
B3LYP/6-311++G(2d,2p)	1.573	–	–	5l
MP2/6-311++G(d)	1.5758	–	–	5a
CI(SD)	1.571	–	–	5j
CCSD(T)/cc-pV(5,Q)Z+aug(H,F)	1.5808	–	–	5d
CCSD(T)/MT(ae)	1.5499	–	–	5d
Exp: microwave[a]	1.56389	–	–	3c
$(FLi)_4$				
BP86/TZ2P	1.859	2.483	2.761	This work
HF/6-31G	1.828	2.484	2.667	5(i,k)
MP2	1.824	–[b]	–[b]	5g
FNa				
BP86/TZ2P	2.000	–	–	This work
HF/6-311++G(2d,2p)	1.929	–	–	5l
B3LYP/6-311++G(2d,2p)	1.943	–	–	5l
MP2/6-311++G(d)	1.9420	–	–	5a
Exp: microwave[a]	1.92595	–	–	3d
Exp: electron diffraction[a]	1.917(2)	–	–	3a
$(FNa)_4$				
BP86/TZ2P	2.241	3.095	3.241	This work
HF/ECPs	2.06	–[b]	–[b]	5e
FK				
BP86/TZ2P	2.296	–	–	This work
HF/6-31+G**	2.222	–	–	5h
MP2(FU)/6-31+G**	2.228	–	–	5h
Exp: microwave[a]	2.17144	–	–	3g
Exp: electron diffraction[a]	2.161(4)	–	–	3a
$(FK)_4$				
BP86/TZ2P	2.548	3.664	3.540	This work
FRb				
BP86/TZ2P	2.397	–	–	This work
HF/6-31+G**	2.367	–	–	5h
MP2(FU)/6-31+G**	2.378	–	–	5h
Exp: microwave[a]	2.26554	–	–	3h
Exp: electron diffraction[a]	2.268(8)	–	–	3a
$(FRb)_4$				
BP86/TZ2P	2.650	3.820	3.673	This work

[a] r_e values.
[b] Not specified in reference.

the T_d symmetric alkalimetal fluoride tetramers increases monotonically if one descends the periodic table from 1.859 (Li) to 2.241 (Na) to 2.548 (K) to 2.650 Å (Rb), similar to the monomers, but at somewhat larger values than in the latter. A remarkable structural phenomenon is the change of relative size of the fluoride tetrahedron and the metal cluster if one goes from sodium to potassium. Thus, for Li and Na, the F_4 unit is, as would be expected, inside the M_4 cluster (i.e. F—F > M—M) similar to the situation found for methyllithium and methylsodium tetramers.[6b] Strikingly, however, for the heavier alkalimetals K and Rb, the F_4 unit is inside the M_4 cluster (i.e. F—F < M—M), as illustrated by Figure 1. This is unprecedented in the methylalkalimetal tetramers in which the metal cluster is always smaller than the surrounding cage of four methyl groups, also for potassium and rubidium. This can be ascribed to the larger steric demand of a CH_3 group as compared to F. An interesting question, in connection with this observation, is whether the same phenomenon still occurs for the corresponding alkalimetalchloride tetramers. Preliminary results show that this is not the case: the Cl_4 unit in cubic M_4Cl_4 is always larger than the M_4 cluster for all four alkalimetals: Li, Na, K, and Rb.

We are not aware of any experimental data on the geometry parameters of alkalimetal fluoride tetramers. This prevents a comparison of structural trends found by us with experiment. Other theoretical work is also limited to Hartree–Fock[5(i,k)] and MP2[5g] geometries for $(FLi)_4$ and a Hartree–Fock[5e] geometry of $(FNa)_4$ (Table 1). The trends that evolve from the Hartree–Fock $(FM)_4$ structures agree with ours, i.e., the F—M bond elongates from Li to Na, and for both metals, the M_4 cluster is smaller than and surrounded by the F_4 tetrahedron.

Thermochemistry

Monomers

The thermochemical results of our BP86/TZ2P calculations are collected in Tables 2 (monomers) and 3 (tetramers). Homolytic dissociation of the F—M bond in alkalimetal fluoride monomers (i.e., FM $\rightarrow F^{\bullet} + M^{\bullet}$) is favored over heterolytic or ionic dissociation (i.e., FM $\rightarrow F^{-} + M^{+}$) for all alkalimetal fluoride monomers with heterolytic bond dissociation enthalpies (BDE = $-\Delta H$ in Table 2) being 1.2–1.4 times higher than the homolytic ones. This is because charge separation is energetically highly unfavorable in the gas phase. The F—M bond strength decreases markedly if one goes from lithium to the heavier alkalimetals, and is more or less constant along the latter. For example, the homolytic BDE is −135.7, −112.1, −114.0, and −114.1 kcal/mol along M = Li, Na, K, and Rb (see ΔH_{homo} in Table 2). This finding is remarkable because, as explained in Analysis of the F—M Bond in Alkalimetal Fluoride Monomers section, for an ionic bond, one would expect an increase of the bond strength if the metal becomes more electropositive, i.e. along Li—Rb. Thus, the present results indicate covalent character of the

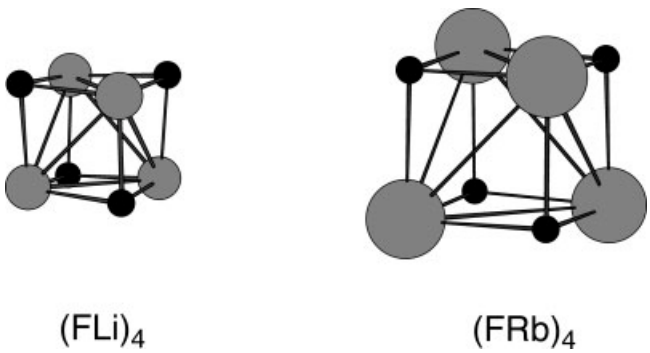

Figure 1. Structures (on scale) of alkalimetal fluoride tetramers for lithium and rubidium (for numerical results, see Table 1).

Table 2. Homolytic and Heterolytic F—M Bond Strength (in kcal/mol) of Alkalimetal Fluoride Monomers.

Method[a]	Bond energies[b]		Bond enthalpies[c]		Ref.
	ΔE_{homo}	ΔE_{hetero}	ΔH_{homo}	ΔH_{hetero}	
FLi					
BP86/TZ2P	−136.0	−185.8	−135.7	−185.5	This work
CI(SD)	−139.7	–	–	–	5j
CBS-Q[e]	−136.6		–	–	5f
B3LYP/6-311+G(2df,p)	–	−185.2	–	–	5b
MP2	–	−178.6	–	–	5c
Exp: flame photometry[d]	−136.1±8.1	–	–	–	3e
Exp: thermochemical[d]	−137.4	–	–	–	3f
Exp.	–	−184.7	–	–	5c
FNa					
BP86/TZ2P	−112.0	−157.0	−112.1	−157.1	This work
CI(SD)	−115.1	–	–	–	5j
B3LYP/6-311+G(2df,p)	–	−151.1	–	–	5b
MP2	–	−154.4	–	–	5c
Exp: flame photometry[d]	−121.1±6.9	–	–	–	3e
Exp: thermochemical[d]	−113.9	–	–	–	3f
Exp.	–	−154.5	–	–	5c
FK					
BP86/TZ2P	−113.8	−138.4	−114.0	−138.6	This work
CI(SD)	−116.9	–	–	–	5j
B3LYP/6-311+G(2df,p)	–	−139.3	–	–	5b
Exp: flame photometry[d]	−116.9±8.1	–	–	–	3e
Exp: thermochemical[d]	−117.6	–	–	–	3f
BP86/TZ2P	−113.9	−133.8	−114.1	−134.0	This work
CI(SD)	−116.2	–	–	–	5j
Exp: flame photometry[d]	−119.9±8.1	–	–	–	3e
Exp: thermochemical[d]	−116.2	–	–	–	3f

[a]Energy and structure obtained at the same level of theory.
[b]Zero K electronic energies.
[c]298.15 K enthalpies.
[d]D_o values. ZPE for FLi, FNa, FK, and FRb are calculated to be 1.2, 0.7, 0.6, and 0.5 kcal/mol, respectively, at the BP86/T2ZP level of theory.

highly polar F—M bond. We wish to point out however that a comparison with an earlier investigation[6] of the C—M bond in methylalkalimetal monomers CH_3M shows that the behavior of the F—M bond is clearly less covalent than that of the C—M bond. We come back to this in Analysis of the F—M Bond in Alkalimetal Fluoride Monomers section.

The results of our BP86/TZ2P computations agree well with those of experimental and other theoretical studies, which all find a sizeable decrease in homolytic bond strength on moving from Li to Na followed by only slight changes along Na—Rb (Table 2). For example, the homolytic bond dissociation energies ΔE_{homo} at CI(SD) are −139.7, −115.1, −116.9, and −116.2 kcal/mol along Li—Rb as compared to −136.0, −112.0, −113.8, −113.9 kcal/mol at BP86/TZ2P. The corresponding experimental thermochemical D_0 values are −137.4, −113.9, −117.6, and −116.2 kcal/mol.

Tetramers

The tetramerization enthalpies of the alkalimetal fluorides (i.e., ΔH_{tetra} associated with the reaction 4 FM $\rightarrow$(FM)$_4$, see Table 3) become systematically less stabilizing if one descends the periodic table, i.e., from −166.1 (Li) to −153.4 (Na) to −142.1 (K) to −133.3 kcal/mol (Rb). These ΔH_{tetra} are all significantly more stabilizing than the corresponding values for the methylalkalimetal molecules CH_3M that amount to −120.3, −73.5, −82.5, −87.1 kcal/mol.[6b] Note also that the tetramerization energy decreases much more pronouncedly going from Li to Na in case of the methylalkalimetals than for the alkalimetal fluorides.

There are no experimental tetramerization energies for alkalimetal fluorides, and also theoretical data are provided only for lithium fluoride. Thus, we cannot compare the trends we find along Li—Rb with those of other studies. The HF/6-31+G* value[5k] of −187.8 kcal/mol for the tetramerization energy ΔE_{tetra} is about 19 kcal/mol more stabilizing than the BP86/TZ2P value of −169.1 kcal/mol (Table 3). The discrepancy with our DFT values is however substantially reduced, i.e., to 7 kcal/mol, if correlation is introduced in the *ab initio* computations at the MP2 level[5g] at which ΔE_{tetra} amounts to −176.5 kcal/mol.

Table 3. Tetramerization Energies and Enthalpies (in kcal/mol) of Alkalimetal Fluoride Monomers.

Method[a]	ΔE_{tetra}[b]	ΔH_{tetra}[c]	Ref.
FLi			
BP86/TZ2P	−169.1	−166.1	This work
HF/6-31+G*	−187.8	–	5k
MP2	−176.5	–	5g
FNa			
BP86/TZ2P	−156.1	−153.4	This work
FK			
BP86/TZ2P	−144.8	−142.1	This work
FRb			
BP86/TZ2P	−135.8	−133.3	This work

[a]Energy and structure obtained at the same level of theory.
[b]Zero K electronic energies.
[c]298.15 K enthalpies.

Analysis of the F—M Bond in Alkalimetal Fluoride Monomers

The analyses of the electronic structure and bonding mechanisms in alkalimetal fluoride monomers reveal not only an extremely high polarity but also suggest a predominant ionic bonding mechanism for the F—M bond (Table 4 and Fig. 2); the covalent character of the F—M bond is strongly reduced when compared to that of the C—M bond.[6] In the first place, for all four alkalimetals, the F—M bond is characterized by a rather weak mixing between the fluorine $2p_\sigma$ AO and the alkalimetal ns AO in the $2p_\sigma$ + ns electron-pair bonding combination (Fig. 2). In fact, the electron-pair bonding $2p_\sigma$ + ns combination is polarized so strongly toward fluorine that it can be better conceived as a distorted fluorine $2p_\sigma$ lone pair: in terms of Gross Mulliken contributions, (The description of the MO in terms of fragment MO coefficients instead of Gross Mulliken contributions yields the same picture, but it has the disadvantage of not being normalized, that is, the figures do not add up to 1 (or to 100%)).[18] the composition is ∼93% $2p_\sigma$ + 4% ns (Fig. 2). In the case of lithium hydride, the situation is 93% 1s + 3% 2s. There is in addition some bonding admixture of the metal np_σ AO, which in the case of Li contributes 2%. This mixing is clearly less pronounced than for the C—M bond in methylalkalimetal monomers (∼70% $2a_1$ + 25% ns),[6b] in line with the F—M bond being more polar than the C—M bond. In terms of mixing coefficients, this is 0.95 $2p_\sigma$ + 0.27 2s (+0.22 $2p_\sigma$) for F—Li, which has to be compared with the more balanced situation of 0.72 $2a_1$ + 0.53 2s (+ 0.32 $2p_\sigma$) for H_3C—Li.[6b]

The reduced F—M mixing suggests that the stabilization due to $2p_\sigma$ + ns overlap and orbital interaction is less important for this bond, which is confirmed by further analyses. The F—M bond interaction-matrix elements $F_{bond} = \langle 2p_\sigma|F|ns\rangle$ between the two SOMOs range from −27.4 (Li) to −27.4 (Na) to −15.3 kcal/mol (K) (Table 4; F is the effective one-electron Hamiltonian or Fock operator evaluated with the fully converged SCF density of the molecule). These F_{bond} values are not only much smaller than the corresponding ones for the C—M bond [i.e., −66.5 (Li), −60.9 (Na), −43.7 kcal/mol (K)],[6b] they also decrease much less along this series of metal atoms.

Table 4. Analysis of the Fluorine–Metal Bond between F· and M· in Alkalimetal Fluoride Monomers.[a]

	F—Li	F—Na	F—K	F—Rb
Bond energy decomposition (in kcal/mol)				
ΔE_σ	−168.4	−132.8	−131.0	−131.7
ΔE_π	−1.0	0.8	0.6	0.7
ΔE_{oi}	−169.4	−132.0	−130.4	−131.0
ΔE_{Pauli}	50.1	34.5	28.3	29.2
ΔV_{elstat}	−16.7	−14.5	−11.7	−12.1
$\Delta E_{int} = \Delta E_{homo}$	−136.0	−112.0	−113.8	−113.9
Fragment orbital overlaps $\langle F\|M\rangle$[b]				
$\langle 2s\|ns\rangle$	0.26	0.22	0.18	0.17
$\langle 2p_\sigma\|ns\rangle$	0.09	0.09	0.06	0.05
$\langle 2p_\sigma\|np\pi\rangle$	0.20	0.15	0.11	0.10
Fragment orbital interaction matrix elements $\langle F\|F\|M\rangle$[b,c] (in kcal/mol)				
$\langle 2p_\sigma\|F\|ns\rangle$	−27.4	−27.4	−15.3	[c]
Fragment orbital populations[b] (in electrons)				
F				
$2p_\sigma$	1.88	1.85	1.87	1.88
M				
ns	0.03	0.07	0.07	0.06

[a]At BP86/TZ2P. See Bond Energy Decomposition section for explanation of energy terms.
[b]n = 2, 3, 4, and 5 for M = Li, Na, K, and Rb, respectively.
[c]Computed with the fully converged SCF density of FM. Cannot yet be computed for Rb for technical reasons.

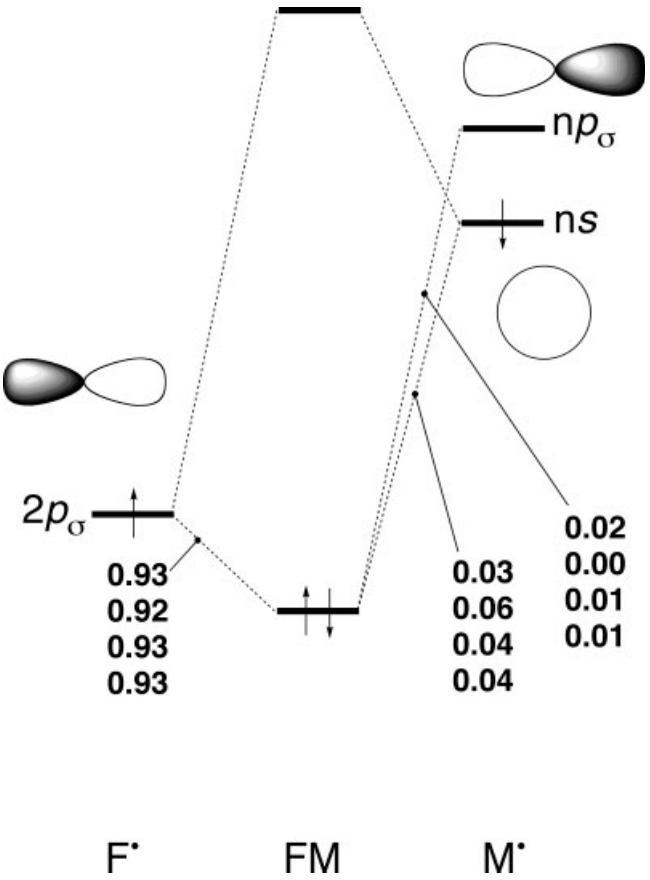

Figure 2. Orbital interaction diagram for FM with Gross Mulliken contributions at BP86/TZ2P of F• and M• fragment orbitals to the F—M electron-pair bonding MO for M = Li, Na, K, and Rb.

The F—M and C—M trends in F_{bond} values can be directly related to the same trends in the corresponding bond overlap integrals S_{bond}: for F—M, the values of $S_{bond} = \langle 2p_\sigma | ns \rangle$ amount to only 0.09, 0.09, 0.06, and 0.05 along F—Li, F—Na, F—K, and F—Rb (Table 4) while, for C—M, the corresponding values $S_{bond} = \langle 2a_1 | ns \rangle$ are 0.31, 0.28, 0.21, and 0.19 for C—Li, C—Na, C—K, and C—Rb.[6b] The decrease in overlap along the series is caused by the metal ns AOs becoming more diffuse and extended along this series, leading to smaller optimum overlap at longer bond distance. The F—M bond distance also increases along Li—Rb because of the increasing number of metal core shells that enter into Pauli repulsion with closed shells on the methyl fragment. For a discussion on how the interplay of bonding and repulsive orbital interactions determines bond lengths.[18] The F—M overlap is smaller because the fluorine $2p_\sigma$ SOMO is more compact and less directed toward the diffuse alkalimetal AOs than the "sp^3-like" methyl 2a1 SOMO.

The difference between F—M and C—M bonds becomes even larger if we take into account that the orbital-energy gap between the SOMOs across F—M is much larger than that across C—M (Fig. 3).[6b] We recall that the stabilization $\Delta\varepsilon$ of our electron-pair bonding $2p_\sigma + ns$ combination with respect to $\varepsilon(2p_\sigma)$ is, in second order (and neglecting the effect of other occupied and virtual orbitals!), given by $\langle 2p_\sigma | F | ns \rangle 2/\varepsilon(2p_\sigma) - \varepsilon(ns)$, that is, the interaction-matrix element squared and divided by the difference in orbital energies.[19] Thus, the stabilization $\Delta\varepsilon$ is inversely proportional to the orbital-energy gap and should therefore be significantly smaller for F—M than for C—M bonds. This is indeed the case: according to the aforementioned approximate relationship, the stabilization $\Delta\varepsilon$ of the F—M "electron-pair bonding combination" relative to the fluorine, $2p_\sigma$ AO is only 3.1 kcal/mol for the F—Li bond, 3.0 kcal/mol for the F—Na bond, and 0.9 kcal/mol for the F—K bond [see $\varepsilon(2p_\sigma)$, $\varepsilon(ns)$, and $\langle 2p_\sigma | F | ns \rangle$ values in Fig. 3 and Table 4). The corresponding values for the C—M bond are a sizeable 67, 48, and 18 kcal/mol for C—Li, C—Na, and C—K.[6b]

The exact (within our KS-MO approach) value of the orbital interactions ΔE_{oi} are enormously stabilizing with values of −169.4, −132.0, −130.4, and −131.0 kcal/mol along the F—Li, F—Na, F—K, and F—Rb bonds (Table 4). Compare this with the corresponding, much less stabilizing values of −63.1, −42.2, −38.4, and −42.2 kcal/mol for the C—Li, C—Na, C—K, and C—Rb bonds.[6b] The small bond-overlap-derived stabilization $\Delta\varepsilon$ of a few kcal/mol suggests that the strongly stabilizing F—M orbital interactions (at variance with the situation for the C—M bond, cf. ref. 6b) are not caused by such a covalent bonding mechanism, schematically shown in **6**, later:

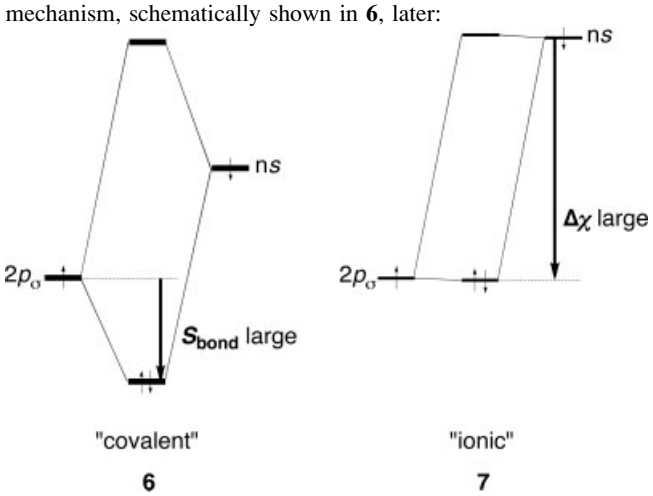

The strongly stabilizing F—M orbital interactions ΔE_{oi} are predominantly caused by an ionic bonding mechanism, which is schematically shown in **7**, earlier. They are directly related to the large difference in electronegativity across the F—M bond, that is,[20] the low energy of the fluorine (−13.8 eV, Fig. 3) as compared to the methyl SOMO (−6.5 eV). As a result of this large difference in orbital energies, the electron that drops into the electron-pair bonding combination (nearly entirely fluorine $2p_\sigma$ in the case of F—M) experiences a sizable stabilization. Note again that compared to the ΔE_{oi} values of −130 to −169 kcal/mol, the estimated contribution of only a few kcal/mol from bond-overlap-derived stabilization $\Delta\varepsilon$ is of minor importance.

The relatively constant value of the bond energy and orbital interactions along F—Na, F—K, and F—Rb is in line with the correspondingly small changes in the basic bonding parameters, in particular, the $\varepsilon(2p_\sigma) - \varepsilon(ns)$ energy gap and the (anyway less important) bond overlap (Fig. 3 and Table 4). The pro-

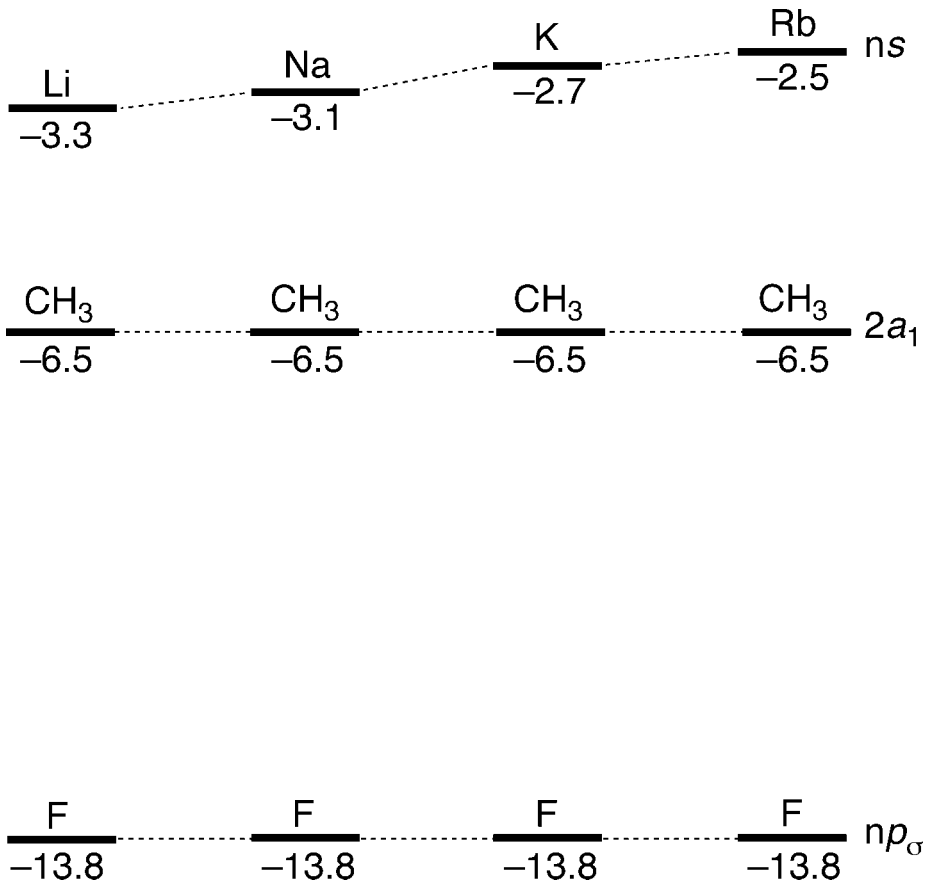

Figure 3. Energies ε (in eV) of the SOMOs of fluorine, (pyramidal) methyl, and alkalimetal radicals at BP86/TZ2P.

nounced decrease of orbital interactions ΔE_{oi} (and thus the bond strength ΔE_{homo}) from F—Li to F—Na may be partially ascribed to the loss of the small, stabilizing contribution of the lithium $2p_\sigma$ AO (Fig. 3). However, the main reason is probably the drastic reorganization in the charge distribution, as this highly polar bond is formed from two neutral atoms. This phenomenon, which is normally left out in qualitative MO considerations, causes a destabilization of the bonding electron-pair, as each of the two electrons go from an initially neutral atom (F and M) to a situation in which they occupy the $2p_\sigma$ AO in a strongly anionic fluorine atom. This destabilization is balanced by the proximity of the strongly positively charged metal atom which stabilizes the excess negative charge on fluorine. This stabilization is most effective, leading to the strongest orbital interactions, for the positively charged lithium, because this atom is most compact and approaches most closely the negatively charged fluorine atom. Unfortunately, the above "charge effect" cannot be straightforwardly quantified.

In conclusion, the F—M bond is not only extremely polar (*vide infra*), but also is mainly provided by the ionic bonding mechanism associated with the metal electron dropping into the fluorine $2p_\sigma$ SOMO. Bond-overlap-derived stabilization plays a minor role only. Thus, an alkalimetal fluoride molecule may be conceived as a cation-stabilized fluoride anion.

Charge Distribution

The metal atomic charge in FM increases from Li to Na and remains essentially constant from Na to Rb according to both the VDD and Hirshfeld method (Table 5). The VDD method,

Table 5. Metal Atomic Charge (in e) and Dipole Moment μ (in D) of Alkalimetal Fluoride Monomers and Tetramers.[a]

	FLi	FNa	FK	FRb	$(FLi)_4$	$(FNa)_4$	$(FK)_4$	$(FRb)_4$
VDD	0.544	0.625	0.631	0.645	0.346	0.453	0.441	0.426
Hirshfeld	0.587	0.626	0.662	0.670	0.417	0.484	0.533	0.537
μ	6.511[b]	8.293[c]	9.510[d]	9.877[e]	0	0	0	0

[a]At BP86/TZ2P.
[b]Exp: 6.327 ± 0.001 D, see ref. 3c.
[c]Exp: 8.156 ± 0.001 D, see ref. 3b.
[d]Exp: 8.60 ± 0.09 D, see ref. 3g.
[e]Exp: 8.80 ± 0.10 D, see ref. 3h.

for example, yields values of $+0.544e$, $+0.625e$, $+0.631e$, and $+0.645e$ along the series. In agreement with this and the increasing F—M bond length, the dipole moment μ increases steeply at first and then more moderately: $\mu = 6.5$, 8.3, 9.5, and 9.9 D along Li, Na, K, and Rb (Table 5). These values indicate that the F—M bond is clearly more polar than the C—M bond for which smaller metal atomic charges (VDD: $+0.386e$, $+0.351e$, $+0.428e$, and $+0.466e$) and dipole moments (5.6, 5.2, 6.9 and 7.7 D) have been computed.[6b] This reflects the stronger polarization of the electron-pair bonding combination of the SOMOs toward the electronegative fragment in the F—M than in the C—M bond, which has its origin in the larger electronegativity difference across the former bond (*vide supra*). This is illustrated by **8a** and **8b**, respectively.

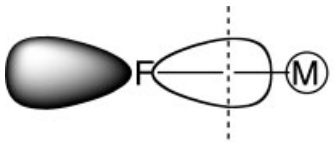

8a

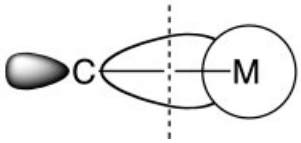

8b

The dashed lines in **8** represent the bond midplanes. They are shown to facilitate recognizing the increased shift of electronic charge away from the metal and toward the electronegative atom in the F—M bond **8a**.

Note that the above mechanism does not account for the increasing metal atomic charges within the F—M series because, as pointed out earlier, the composition of the electron-pair bonding combination changes hardly and is more or less constantly 93% $2p_\sigma$ + 5% ns (Fig. 2). This is, by the way, in line with the relatively small variation in electronegativity along Li—Rb as compared to that going from F to CH_3. The origin of the increasing extent of charge separation is that the fluorine atom moves still farther away from the metal atom as the latter becomes larger along Li—Rb. Thus, the negative charge gained by fluorine due to the formation of the polar $2p_\sigma$ + ns electron-pair bond penetrates less into the region of the metal atom and is increasingly associated with the fluorine atom. This is illustrated in **9**, which shows a polar electron-pair bonding combination of fixed composition for a short (**9a**) and a long (**9b**) F—M bond (the dashed line indicates the bond midplane).

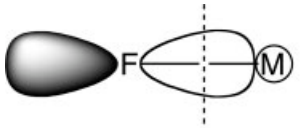

9a

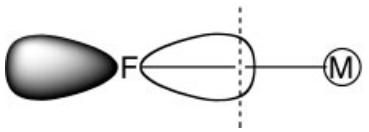

9b

The aforementioned combination is nicely corroborated by the following numerical experiment. We have increased the F—Li distance stepwise from the equilibrium bond length of FLi to that of FNa, FK, and FRb. This causes the interaction energy in LiF to decrease, of course, and the $2p_\sigma$ + 2s electron-pair bonding combination becomes slightly less polarized. Yet, the charge separation increases both according to VDD and Hirshfeld. For example, the VDD atomic charge of lithium in FLi increases from $+0.544e$ (Table 5) to $+0.596e$ to $+0.636e$ to $+0.645e$ (not shown in Table), thus closely following the alkalimetal atomic charges in the FM molecules along Li—Rb (Table 5).

Heterolytic Bond Dissociation

So far, we have examined the extent of orbital mixing, its importance for trends in the bond strength, and the polarity or charge separation in the F—M bond. Another criterion for classifying the F—M bond as ionic is the reduced intrinsic preference for dissociating homolytically as compared to dissociating heterolytically (*vide supra*). To enable a quantitative comparison with other bonds, we have computed the ratio of $\Delta E_{\text{hetero}}/\Delta E_{\text{homo}}$ as a measure for this preference, using bond energy values from Table 2. The $\Delta E_{\text{hetero}}/\Delta E_{\text{homo}}$ ratios of FLi, FNa, FK, and FRb are 1.4, 1.4, 1.2, and 1.2, respectively. These values are significantly smaller than the $\Delta E_{\text{hetero}}/\Delta E_{\text{homo}}$ ratios of the corresponding C—M bonds of the methylalkalimetal monomers (3.9, 5.0, 4.9, and 5.0) and that of the C—H bond in methane (3.8), which is in general considered a classical covalent bond.[6b] Thus, the F—M bond behaves clearly more ionic than the C—M bond (and the C—H bond) also in the sense that heterolytic dissociation (as compared to homolytic dissociation) has become energetically much less unfavorable.

It is instructive to carry out an ionic analysis of the F—M bond, that is, a bond energy decomposition of the interaction between F^- and M^+ in FM (Table 6) and to compare this with the analysis of the interaction between $F^\bullet$ and $M^\bullet$ in the same molecule (Table 4). In the ionic approach, the classical electrostatic attraction ΔV_{elstat} becomes the dominant bonding term with values that vary from −204.1 to −172.0 to −153.7 to −150.4 kcal/mol along Li—Rb (Table 6). The decrease in ΔV_{elstat} is due to the increasing F—M bond distance along this series. Note the enormous increase in ΔV_{elstat} compared to the

Table 6. Analysis of the Fluorine–Metal Bond between F^- and M^+ in Alkalimetal Fluoride Monomers.[a]

	F—Li	F—Na	F—K	F—Rb
ΔE_σ	−6.9	−6.0	−6.3	−7.8
ΔE_π	−10.1	−6.6	−7.5	−8.2
ΔE_{oi}	−17.0	−12.6	−13.8	−16.0
ΔE_{Pauli}	35.3	27.6	29.1	32.6
ΔV_{elstat}	−204.1	−172.0	−153.7	−150.4
$\Delta E_{\text{int}} = \Delta E_{\text{hetero}}$	−185.8	−157.0	−138.4	−133.8

[a]At BP86/TZ2P.

homolytic approach (compare Tables 4 and 6) is, as such, no indication for ionic character. It is due to the energetically unfavorable charge separation that we enforce by our choice to completely transfer one electron from one of the constituting fragments of FM to the other. This occurs for any other bond that dissociates heterolytically, e.g., also C—H and C—C.

The electrostatic term ΔV_{elstat}, in particular, the trend therein along Li—Rb, nicely illustrates the model of a cation-stabilized fluoride that we invoked to rationalize the trend in orbital interactions ΔE_{oi} of the homolytic approach (*vide supra*). Transferring an electron from an isolated alkalimetal (= ionization energy, IE) to an isolated fluorine atom (= negative electron affinity, −EA) is endothermic by 49.8 (Li), 45.0 (Na), 24.6 (K), and 19.9 kcal/mol (Rb). In other words, the energy required to remove an electron from M is not compensated by the gain in energy associated with accomodating the electron on F (i.e., IE − EA > 0), despite the fact that the orbital energy of the (neutral) fluorine SOMO is lower than that of the (neutral) alkalimetal SOMO. What happens is that the fluorine $2p_\sigma$ is significantly destabilized by the net negative charge, as the extra electron is accommodated. However, if the F and M are in proximity, i.e., in the FM molecule, the net negative electrostatic potential of fluoride is compensated by the stabilizing net positive potential of the alkalimetal cation. This provides a stabilizing contribution to the $2p_\sigma$ (+ ns) orbital and the charge transfer associated with the orbital interactions in the homolytic approach becomes overall stabilizing again. We stress here that while this electrostatic interaction is related to the term ΔV_{elstat} of the heterolytic approach, it is definitely not the same. In fact, it must be much smaller. This is because the heterolytic ΔV_{elstat} refers approximately to bringing an electron from F^- and M^+ from infinity together at FM, while the electrostatic component in the homolytic ΔE_{oi} refers approximately to the same process plus the cost in energy to remove the electron first from M and to bring it to F.

Analysis of Monomer–Monomer Interactions in FM Tetramers

To understand the stability of the alkalimetal fluoride tetramers toward dissociation into the four monomers, we have analyzed the interaction between these monomers in the tetramer. The decomposition of the tetramerization energy, shown in Table 7, reveals that the electrostatic attraction ΔV_{elstat} is the dominant bonding force. This term decreases from −285.4 (FLi) to −247.2 (FNa) and then more moderately to −234.2 (FK); thereafter, it increases slightly to −245.4 kcal/mol (FRb). This correlates well with the F—M bond length, which increases more strongly from Li to K, causing the electrostatic interactions to become weaker. From K to Rb, the F—M bond expands only slightly (from 2.548 to 2.650 Å, Table 1) and the increase in charge separation eventually causes a slight increase in ΔV_{elstat}.

The orbital interactions ΔE_{oi} between the FM monomers, although much smaller than ΔV_{elstat}, are still important for the cohesion between the monomers, with values ranging from −55.4 kcal/mol for the lithium fluoride tetramer to −33.9 kcal/mol for the sodium fluoride tetramer (Table 7). Note that these orbital interactions do not involve the formation of an electron-pair bond. They are mainly provided by donor–acceptor interactions of occupied σF—M and F lone-pair orbitals (mainly located on F) with unoccupied σ*F—M orbitals (mainly located on M) of the monomers. Consequently, tetramerization reduces the charge separation, because the donor–acceptor orbital interactions cause charge transfer from F to M. This is also confirmed by the VDD and Hirshfeld atomic charges, which are consistently smaller in $(FM)_4$ than in FM (Table 5). The same phenomenon has also been observed for the corresponding methylalkalimetal systems.[6b] The net interaction energy ΔE_{int} between FM monomers decreases steadily from −195.2 to −149.5 kcal/mol along Li—Rb. This trend is preserved in the overall tetramerization energies and enthalpies (Tables 3 and 7). Tetramerization is significantly more stabilizing for alkalimetal fluorides FM (ΔH_{tetra} = −166.1 to −133.3 kcal/mol along Li—Rb, Table 3) than for methylalkalimetal molecules CH_3M (ΔH_{tetra} = −120.8 to −87.1 kcal/mol, ref. 6b), among others because of less Pauli (steric) repulsion between monomers in case of the former.

Table 7. Monomer–Monomer Bond Energy (in kcal/mol) Decomposition for Alkalimetal Fluoride Tetramers.[a]

	$(FLi)_4$	$(FNa)_4$	$(FK)_4$	$(FRb)_4$
ΔE_{oi}	−55.4	−33.9	−35.0	−37.9
ΔE_{Pauli}	145.6	106.0	109.1	133.8
ΔV_{elstat}	−285.4	−247.2	−234.2	−245.4
ΔE_{int}	−195.2	−175.1	−160.1	−149.5
ΔE_{prep}	26.1	19.0	15.3	13.7
ΔE_{tetra}	−169.1	−156.1	−144.8	−135.8

[a]At BP86/TZ2P.

Covalency and Ionicity: Physical Interpretation and Criteria

Earlier we have discussed the nature of a series of F—M bonds, in particular, the extent to which they behave "ionically" as opposed to "covalently." We will not discuss here the concept of "covalency" in its quality of donor–acceptor orbital interactions, i.e., as opposed to electrostatic interactions between closed-shell molecular fragments, such as DNA bases in Watson–Crick and other base pairs. For an extensive discussion of this issue, the reader is referred to ref. 16a.[16,21] In the following, we elaborate more explicitly on these concepts as such. What is exactly meant with the covalency[22] and ionicity of a bond? And to what extent can these properties be defined in a quantitative and physically meaningful manner? Let us begin with summarizing some of the quantities that we have analyzed earlier in order to examine the ionicity (or covalency) of the F—M bonds: (i) the magnitude and trend in the orbital interaction ΔE_{oi}; (ii) the composition of the wavefunction (or the electron-pair bonding MO) in terms of F and M contributions; and (iii) the charge separation across the F—M bond. These are three, to some extent, orthogonal aspects of the property of ionicity. They are determined by three main factors: (i) the bond overlap S_{bond} or, more precisely, the interaction matrix element F_{bond}, between the SOMOs of F and M; (ii) the electronegativity difference $\Delta\chi$ or, more pre-

cisely, the difference in SOMO energies of F and M; and (iii) the bond distance F—M.

One approach of classifying a bond as covalent or ionic is by determining which of the aforementioned factors dominates the energetics, that is, the trend in F—M bond energies. Here, the bond overlap is the factor that can be associated with covalent character: if it dominates the behavior, e.g., trends in bond energies, the bond can be considered covalent (e.g., the C—M bond).[6b] On the other hand, the bond may be conceived ionic if the electronegativity difference determines much of its behavior, as is the case for the F—M bond in this study. Not only is this bond highly polar in terms of its charge distribution (dipole moment and atomic charges), but also in terms of its bonding mechanism. This is important in view of our previous finding that despite a high polarity the C—M bond has unexpectedly substantial covalent character (which is essential for understanding trends in bond strengths). Thus, one must distinguish between covalent or ionic features in the bonding mechanism on one hand and the polarity of the charge distribution on the other hand.[6]

Nevertheless, the polarity of chemical bonds is an important property and is often used as an alternative definition of covalency and ionicity. One approach to quantify the polarity is computing the charge separation across the bond in terms of the charges of the atoms involved. The idea is that a completely covalent bond in a neutral molecule, say A—B, involves neutral atoms (or fragments) A and B, whereas a completely ionic bond, in which one electron is completely transferred, is associated with atoms A^+ and B^- carrying opposite charges of +1.0 and −1.0 electrons, respectively. This can be done in a routine manner. Note, however, that atomic charges cannot be interpreted as absolute bond polarity indicators.[6] The problem originates from the fact that different atomic charge schemes have different scales, that is, the value of the computed charge of one particular atom in a molecule can vary significantly from one method to another. Atomic charges can still gain physical meaning but only in terms of trends, i.e., by comparing relative magnitudes of atomic charges computed consistently with the same method. Only in this way, one can learn if a computed charge should be considered small, corresponding to an essentially covalent bond, or large, indicating increased ionic character. Indeed, the F—Li bond can be classified as more polar (54% ionic) than the H_3C—Li bond (39% ionic) and less polar than the F—Rb bond (65% ionic), but it must be clear to which scale these numbers refer, in this example VDD (see Table 5 and ref. 6b). A similar picture emerges if we use, for example, the Hirshfeld scale, but with different absolute values.

We have recently proposed an alternative method[6b] of quantifying the bond polarity, which is based on the composition of the wavefunction in terms of F and M contributions. In particular, we look at the relative contribution x of the SOMO of one of the fragments, say the more electronegative one (here: the fluorine atom), to the F—M electron-pair bonding MO. This approach is firmly rooted in MO theory and has the advantage over atomic charges that at least the range of values between the purely covalent and ionic situations is well defined.[19] Thus, the purely covalent situation occurs for $x = x_C = 0.5$: the radical electrons of both fragments pair-up in an electron-pair bonding combination of the overall molecule that has equal contributions from either fragment SOMO. The purely ionic situation occurs for $x = x_I = 1$: the unpaired electron of the metal atom is completely transferred to the methyl SOMO which transforms, without admixture of the metal AO, into a lone-pair-like MO in the overall molecule. The percentage covalency C and ionicity I is then defined as in eqs. (6) and (7), respectively, with $I + C = 100\%$.

$$C = \frac{x_I - x}{x_I - x_C} \times 100\% \tag{6}$$

$$I = \frac{x - x_C}{x_I - x_C} \times 100\%. \tag{7}$$

Table 8. Covalency C (in %) of F—M and C—M Bonding in Alkalimetal Fluoride and Methylalkalimetal Monomers.[a]

M	F—M	C—M
Li	14 (12)	60 (60)
Na	16 (15)	58 (58)
K	14 (13)	54 (52)
Rb	14 (12)	58 (55)

[a]At BP86/TZ2P. C is computed with eq. (6) using for x the Gross Mulliken contribution of the fluorine $2p_\sigma$ or the methyl $2a_1$ SOMO to the electron-pair bonding combination (see values in Fig. 2 and ref. 6). Value in parentheses: idem, using for x the Gross Mulliken Population P that the fluorine $2p_\sigma$ or the methyl $2a_1$ SOMO acquire in all occupied MOs of the overall molecule (see values in Table 4 and ref. 6) divided by 2, i.e., $x = P/2$.

In Table 8, we have collected percentages of covalency C of the F—M bonds of our alkalimetal fluoride monomers based on eq. (6), using two ways of computing the fraction x. In the first one, x is the Gross Mulliken contribution of the fluorine $2p_\sigma$ SOMO to the electron-pair bonding combination in the overall molecule (see values in Fig. 2). Thus, we can classify the F—Li bond as clearly more polar (14% covalent, 86% ionic) than the H_3C—Li bond (60% covalent, 40% ionic) and of a similar polarity as the F—Rb bond (14% covalent, 86% ionic). Note that here the difference between F—M and C—M polarity is even more pronounced than according to atomic charges. On the other hand, the trend of increasing polarity along Li—Rb obtained on the basis of atomic charges essentially vanishes if we look at the composition of the electron-pair bonding MO. This difference is caused by the fact that the composition of the electron-pair bonding MO mainly depends on the electronegativity (or SOMO energy) difference, whereas the actual charge separation is, in addition, strongly influenced by the F—M distance (the charge separation increases as the bond becomes longer, see **9a** and **9b**). There are still other ways of computing x, for example, on the basis of the Gross Mulliken population P (see values in Table 4) that the fluorine $2p_\sigma$ SOMO acquires in all occupied MOs of the overall molecule ($x = P/2$: see values in parentheses in Table 8), or on the basis of fragment MO coefficients (not shown in Table 8). Note that the particular values of C and I depend on how x is computed. One must be aware that this introduces again a certain arbitrariness making C and I semiquantitative rather than quanti-

tative. Nevertheless, any choice for x produces the same trends in C and I, i.e., a nearly constant extent of covalency of the F—M bond going from Li to the heavier alkalimetals.

Conclusions

The F—M bond in alkalimetal fluorides is not only highly polar (even significantly more so than corresponding C—M bonds in methylalkalimetal oligomers), it is also truly ionic in terms of its bonding mechanism: the stabilization associated with the F—M bond is predominantly caused by the transfer of an electron from a high energy SOMO on the electropositive M to a low-energy SOMO on F. On the other hand, the stabilization that derives from the (small) F—M bond overlap plays no role of importance. Furthermore, the higher F—M compared to the C—M bond strength is entirely due to the larger electronegativity difference across the former bond.

These insights emerge from our quantum-chemical analyses of the alkalimetal fluoride monomers FM and tetramers $(FM)_4$ with M = Li, Na, K and Rb, at BP86/TZ2P. They show that the composition of the F—M wavefunction (in particular the electron-pair bonding MO) is mainly localized on F and that it remains essentially constant along Li—Rb. It is the increasing F—M bond distance that causes the charge separation as well as the dipole moment to become larger in this order. Interestingly, tetramerization reduces the polarity. A striking structural phenomenon is the change of relative size of the fluoride tetrahedron and the metal cluster if one goes from sodium to potassium. For the lithium and sodium fluoride tetramers, the F_4 tetrahedron is larger than and surrounds the M_4 cluster (i.e., F—F > M—M), similar to the situation for the corresponding methylalkalimetal tetramers.[6b] However, at variance with the situation for the corresponding methylalkalimetal tetramers, in the potassium and rubidium fluoride tetramers, the F_4 tetrahedron is smaller than and inside the M_4 cluster (i.e., F—F < M—M).

Our results suggest that, at least for our model systems, it is justified to interpret the covalent and ionic Lewis structures **1** and **2** not only as representations of the charge distribution but also of the bonding mechanism. Accordingly, alkalimetal fluorides must be represented with the ionic structure **2**, whereas methylalkalimetals are best represented by a combination of (or resonance between) the covalent and ionic structures, **1**→**2**.

Acknowledgments

Excellent service by the Stichting Academisch Rekencentrum Amsterdam (SARA) and the Centre de Supercomputació de Catalunya (CESCA) is gratefully acknowledged.

References

1. (a) Lewis, G. N. J Am Chem Soc 1916, 38, 762; (b) Lewis, G. N. J Am Chem Soc 1913, 35, 1448.
2. (a) Hargittai, M. Chem Rev 2000, 100, 2233; (b) Hargittai, M.; Hargittai, I. The Molecular Geometries of Coordination Compounds in the Vapor Phase; Elsevier: Amsterdam, 1997; (c) Zewail, A. H. J Phys Chem A 2000, 104, 5660.
3. (a) Hartley, J. G.; Fink, M. J Chem Phys 1988, 89, 6058; (b) Hollowell, C. D.; Hebert, A. J.; Street, K., Jr. J Chem Phys 1964, 41, 3540; (c) Wharton, L.; Klemperer, W.; Gold, L. P.; Strauch, R.; Gallagher, J. J.; Derr, V. E. J Chem Phys 1963, 38, 1203; (d) Bauer, R. K.; Lew, H. Can J Phys 1963, 41, 1461; (e) Bulewicz, E. M.; Phillips, L. F.; Sugden, T. M. Trans Faraday Soc 1961, 57, 921; (f) Brewer, L.; Brackett, E. Chem Rev 1961, 61, 425; (g) Green, G. W.; Lew, H. Can J Phys 1960, 38, 482; (h) Lew, H.; Morris, D.; Geiger, F. E., Jr.; Eisinger, J. T. Can J Phys 1958, 36, 171.
4. (a) Lintuluoto, M. J Phys Chem A 2000, 104, 6817; (b) Aguado, A.; Ayuela, A.; López, J. M.; Alonso, J. A. Phys Rev B 1997, 56, 15353; (c) Heidenrich, A.; Jortner, J. J Chem Phys 1996, 105, 8523; (d) Redington, R. L. J Chem Phys 1995, 102, 7325; (e) Giraud-Girard, J.; Maynau, D. Z Phys D 1994, 32, 249; (f) Shalabi, A. S.; El Misiery, A. M. Chem Phys Lett 1993, 215, 275; (g) Hodoscek, M.; Solmajer, T. J Am Chem Soc 1984, 106, 1854.
5. (a) Zhuo, S.; Weis, J.; Ju, G. J Chem Phys 2001, 115, 8298; (b) Kim, C. K.; Won, J.; Kim, H. S.; Kang, Y. S.; Li, H. G.; Kim, C. K. J Comput Chem 2001, 22, 827; (c) Lintuluoto, M. J Mol Struct (Theochem) 2001, 540, 177; (d) Breidung, J.; Thiel, W. J Mol Struct (Theochem) 2001, 599, 239; (e) Bonacic-Koutecky, V.; Pittner, J.; Koutecky, J. J Chem Phys 1996, 210, 313; (f) Ochterski, W.; Petersson, G. A.; Wiberg, K. B. J Am Chem Soc 1995, 117, 11299; (g) Ochsenfeld, C.; Ahlrichs, R. Ber Bunsenges Phys Chem 1994, 98, 34; (h) Lambert, C.; Kaupp, M.; Schleyer, P. v. R. Organometallics 1993, 12, 853; (i) Dunlap, B. I. J Chem Phys 1986, 84, 5611; (j) Langhoff, S. R.; Bauschlicher, C. W., Jr.; Partridge, H. J Chem Phys 1986, 84, 1687; (k) Sapse, A.-M.; Raghavachari, K.; Schleyer, P. v. R.; Kaufmann, E. J Am Chem Soc 1985, 107, 6483; (l) Robinson, E. A.; Johnson, S. A.; Tang, T.-H.; Gillespie, R. J Inorg Chem 1977, 36, 3022.
6. (a) Bickelhaupt, F. M.; Solà, M.; Fonseca Guerra, C. J Mol Model 2006, 11, 563; (b) Bickelhaupt, F. M.; Solà, M.; Fonseca Guerra, C. J Chem Theory Comput 2006, 2, 965; (c) Bickelhaupt, F. M.; Solà, M.; Fonseca Guerra, C. Farad Disc (in press).
7. Bitter, T.; Ruedenberg, K.; Schwarz, W. H. E. J Comput Chem 2006, 27.
8. (a) Bickelhaupt, F. M.; Baerends, E. J. In Reviews in Computational Chemistry, Vol. 15; Lipkowitz, K. B.; Boyd, D. B., Eds.; Wiley-VCH: New York, 2000; pp. 1– 86; (b) Poater, J.; Solà, M.; Bickelhaupt, F. M. Chem Eur J 2006, 12, 2902.
9. (a) te Velde, G.; Bickelhaupt, F. M.; Baerends, E. J.; van Gisbergen, S. J. A.; Fonseca Guerra, C.; Snijders, J. G.; Ziegler, T. J Comput Chem 2001, 22, 931; (b) Fonseca Guerra, C.; Snijders, J. G.; te Velde, G.; Baerends, E. J. Theor Chem Acc 1998, 99, 391; (c) Fonseca Guerra, C.; Visser, O.; Snijders, J. G.; te Velde, G.; Baerends, E. J. In Methods and Techniques for Computational Chemistry; Clementi, E.; Corongiu, G., Eds.; STEF: Cagliari, 1995; pp. 305–395; (d) Baerends, E. J.; Ellis, D. E.; Ros, P. Chem Phys 1973, 2, 41; (e) Boerrigter, P. M.; te Velde, G.; Baerends, E. J. Int J Quantum Chem 1988, 33, 87; (f) te Velde, G.; Baerends, E. J. J Comp Phys 1992, 99, 84; (g) Snijders, J. G.; Baerends, E. J.; Vernooijs, P. At Data Nucl Data Tables 1982, 26, 483; (h) Krijn, J.; Baerends, E. J.Fit functions in the HFS method; Internal report (in Dutch); Vrije Universiteit: Amsterdam, 1984.
10. (a) Versluis, L.; Ziegler. T. J Chem Phys 1988, 88, 322; (b) Fan, L.; Ziegler, T. J Chem Phys 1991, 95, 7401; (c) Schreckenbach, G.; Li, J.; Ziegler. T. Int J Quantum Chem 1995, 56, 477.
11. Fan, L.; Versluis, L.; Ziegler, T.; Baerends, E. J.; Ravenek. W. Int J Quantum Chem Symp 1988, 22, 173.
12. (a) Becke, A. D. J Chem Phys 1986, 84, 4524; (b) Becke, A. Phys Rev A 1988, 38, 3098; (c) Perdew, J. P. Phys Rev B 1986, 33, 8822 (Erratum: Phys Rev B 1986, 34, 7406); (d) Fan, L.; Ziegler, T. J Chem Phys 1991, 94, 6057.

13. Atkins, P. W. Physical Chemistry; Oxford University Press: Oxford, 1982.
14. (a) Morokuma, K. J. Chem Phys 1971, 55, 1236; (b) Kitaura, K.; Morokuma, K. Int J Quantum Chem 1976, 10, 325; (c) Bickelhaupt, F. M.; Nibbering, N. M. M.; van Wezenbeek, E. M.; Baerends, E. J. J Phys Chem 1992, 96, 4864; (d) Ziegler, T.; Rauk, A. Inorg Chem 1979, 18, 1558; (e) Ziegler, T.; Rauk, A. Theor Chim Acta 1977, 46, 1.
15. Bickelhaupt, F. M.; van Eikema Hommesqq, N. J. R.; Fonseca Guerra, C.; Baerends, E. J. Organometallics 1996, 15, 2923.
16. (a) Fonseca Guerra, C.; Bickelhaupt, F. M.; Snijders, J. G.; Baerends, E. J. Chem Eur J 1999, 5, 3581; (b) Fonseca Guerra, C.; Handgraaf, J. W.; Baerends, E. J.; Bickelhaupt, F. M. J Comput Chem 2004, 25, 189. (c) Kittel, C. Introduction to Solid State Physics; Wiley: New York, 1986.
17. Hirshfeld, F. L. Theor Chim Acta 1977, 44, 129.
18. Bickelhaupt, F. M.; DeKock, R. L.; Baerends, E. J. J Am Chem Soc 2002, 124, 1500.
19. Albright, T. A.; Burdett, J. K.; Whangbo, M. Orbital Interactions in Chemistry; Wiley: New York, 1985.
20. Mann, J. B.; Meek, T. L.; Allen, L. C. J Am Chem Soc 2000, 122, 2780.
21. (a) Fonseca Guerra, C.; Bickelhaupt, F. M. Angew Chem 1999, 111, 3120; (b) Fonseca Guerra, C.; Bickelhaupt, F. M. Angew Chem Int Ed 1999, 38, 2942; (c) Fonseca Guerra, C.; Bickelhaupt, F. M.; Baerends, E. J. Crystl Growth Design 2002, 2, 239.